P1.22

EFFECTS OF DROP SIZE DISTRIBUTION ON NEXRAD RAIN RATE ESTIMATION

Nazario D. Ramírez-Beltrán*, E. J. Suarez-Vázquez and S. Cruz-Pol
University of Puerto Rico, Mayagüez, Puerto Rico

1. Introduction

The purpose of this research effort is to develop and analyze the droplet size distribution (DSD) for different types of rainfall events, and to measure how the DSD affects the rain-rate radar estimation. The cloud DSD plays a paramount role in the parameterization of cloud microphysics in climate models and plays a crucial role in determining the cloud radiative properties, which is usually obtained by radar and satellite retrieval algorithms. The optical disdrometer is used to collect *in-situ* samples of droplet size, which will be used to develop the parameters of the DSD. A preliminary analysis was conducted throughout of the modified Gamma distribution which is used to represent the cloud DSD. The analysis of the DSD is conducted through the derivation of the distribution moments and their physical interpretation. The analysis includes the discussion of the mean, variance, effective radius, and effective variance of the DSD. It was noted that the effective radius is the ratio of expected volume of water falling in an expected area and the average radius if the arithmetic mean of the droplets and the effective radius is larger than the average of radius. Rain gauges were located in the same place of the disdromater with the purpose of measuring the accumulated rainfall during 5 minutes. NEXRAD reflectivity is compared with the disdrometer reflectivity for different DSDs and only for those events that exhibited more than 500 droplets during the sampling time (five minutes). It was noted that the deviation of reflectivity from radar and disdrometer is smaller for smaller droplets, and larger deviation for larger droplets. Thus, there is an opportunity to develop an algorithm for improving the rain rate radar estimations based on the knowledge of the DSD.

The DSD this is a critical and fundamental information to calibrate a weather radar. The size and the distribution of the water droplets significantly affect the reflectivity and rain rate relationship and consequently the radar rain rate estimation (Tokay et al. 2002).

It is necessary to study the DSD at the surface level in order to understand the behavior of DSD at different elevation levels (Caracciolo et al. 2005). Cloud DSD is usually represented by different mathematical models such as Lognormal, Gamma and/or modified Gamma distribution (Hansen 1971; Nakajima, and King, 1990; Arduini et al., 2005; Yang et al., 2005). However, the modified Gamma distribution is preferred over the Lognormal since the parameters of the modified Gamma distribution are equal to physical parameters which can characterize the scattering of the size distribution (Hansen 1971). Thus, in this research the modified Gamma distribution was used to measure the effects of DSD on radar rainfall estimates.

Reflectivity observations obtained by radar and disdrometer are compared to measure the effect of DSD on radar rain rate estimates. Do to the fact that radar rain rates are calculated with reflectivity data. The experiment was conducted on Puerto Rico (PR), which is a small island located in the Caribbean basin. PR has extremely diverse terrain, and during the rainy season severe rainstorms can develop due to complex orographic attributes. Easterly winds come from the eastern Atlantic almost all year and play an important role bringing humidity into the island and stimulating orographic rainfall over the mountains of PR. Cold fronts dominate the weather pattern during wintertime. Tropical waves occur during the rainy season and frequently generate large amounts of rainfall in the Caribbean basin. These tropical waves are typically the precursor of tropical storms and hurricanes from June to November.

The second section of this paper will describe the equipment and data used for this study. The third section presents a brief description of the Gamma distribution. The fourth section presents the analysis of data. The fifth section presents some conclusions and future work to increase the precision of radar rain rates over the western part of PR.

2. Equipment

In this research three instruments were used to collect the appropriate data and to conduct the analysis: weather radar, optical disdrometer and rain gauges.

2.1 Disdrometer

The surface disdrometer measures the rain drop size distribution (DSD) at the surface and is used to estimate the surface reflectivity, rain rate, and mean rain drop size. The disdrometer due to its measurements accuracy is the preferred instrument to calibrate weather radars. There are two types of instrument: the optical and the impact disdrometers. It has been shown that

**Corresponding authors address:* Nazario D. Ramirez Beltrán, University of Puerto Rico, Dpto. Industrial Engineering, Mayagüez, PR, 00680, e-mail: nazario.ramirez@upr.edu

the optical instrument is more precise than the impact (Clark, et al 2003). Figure 1 shows the PARSIVEL which an optical disdrometer that was used in this research and provides the following features: the drop size, the drop count, and the drop velocity. The instrument uses a laser to measure the number drops and the drop speed by recording the electronic sign when the drop interrupts the sample laser transmission as shown in Figure 2. The electronic interruption allows the instrument to measure the drop diameter, and the speed of interruption is used to estimate the drop speed.

Fig. 1 *The optical Disdrometer***.**

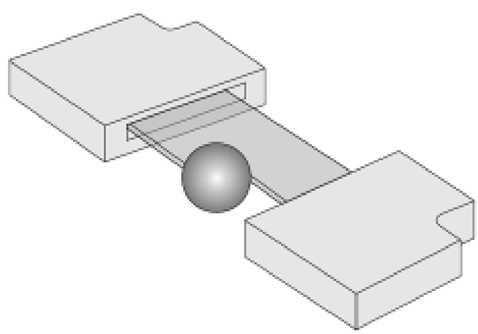

Fig. 2 *An image representation of how the disdrometer takes the data from the rainfall events*

The optical disdrometer also has the capability of estimating the reflectivity at the surface, which is compared with volumetric reflectivity measured by the radar.

2.2 Rain Gauges

A tipping bouquet precipitation with one mm of accuracy was used in this research. Figure 3 shows the data logger and the rain gauge ECRN-50. This instrument is connected to an automatic data logger that recorded the accumulated rainfall every 5 minutes.

A rain gauge was used record the accumulated rainfall during 5 minutes, with an accuracy of 1mm, and essentially it is used to confirm the presence of rainfall events, recorded by the other instruments.

Fig. 3 *The rain gauge and data logger*

2.3 The NEXRAD

The Next Generation Radar (NEXRAD) was installed in Cayey PR in 1997 (18.12°N, 66.08°W, 886.63m elevation). This instrument is also known as a WSR-88D unit, operates at the frequency of 2.7 GHz and the maximum horizontal range is 462.5 km, and the radar scans the entire island every 6 minutes. Figure 4 shows the NEXRAD which retrieves reflectivity with Doppler effects. The NOAA National Severe Storms Laboratory (NSSL) conducted a significant effort to make possible an affordable nationwide operational capture, distribution, and archive of Level II NEXRAD data (Yang et al., 2000). Data level II for Puerto Rico were interrupted for several years (2003-2006); however, the NWS did resume archiving level II data for PR during the summer of 2007. The information used in this research is reflectivity from level II and was collected at the first elevation angle (0.5^{o}) .

Fig. 4 *The NEXRAD installed in PR*

3. The drop size distribution

Data collected from disdrometer were extracted every 5 minutes. The data includes the number of droplets, the reflectivity, and estimation of rain rate. Figure 5 shows an example of the data.

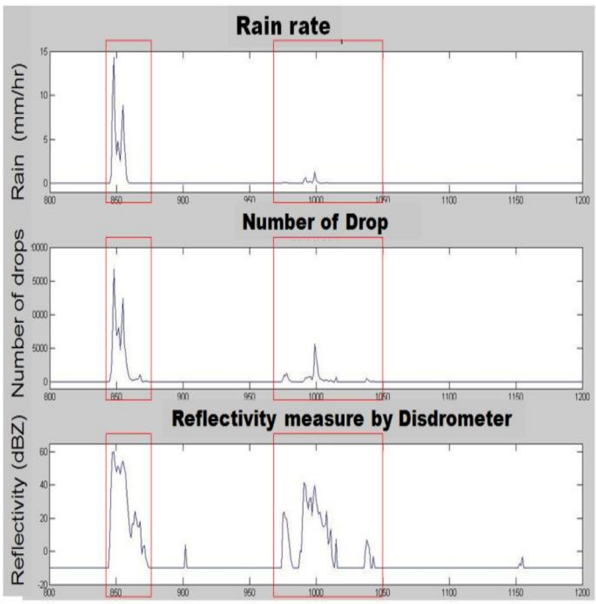

Fig 5. *Data from Disdrometer (June 11-19, 2009)*

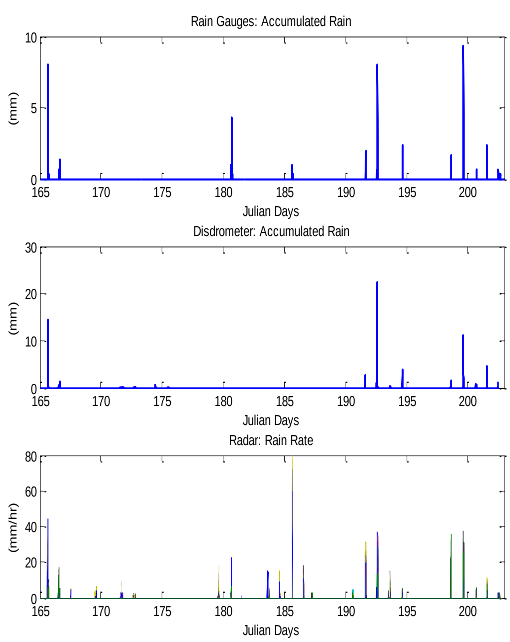

Fig 6. *Two rainfall events recorded by rain gauge, disdrometer and radar (June 11-19, and July 22 2009)*

Figure 6 shows the records of two rainfall events recorded by different instruments. The top panel shows the accumulative rain during 5 minutes from three rain gauges to reduce source of error. The middle panel shows the accumulate rain recorded by the didrometer; it should be noted that disdrometer was not in operation during the period 176 to 190 Julian days. The bottom panel of Fig 6 shows the rain rate recorded by the sixteen pixels of the NEXRAD radar during the occurrence of two rainfall events (June 11-12 and July 22, 2009). This figure shows that the three instruments recorded the two events on the same time interval. However, there are some rainfall amounts in disagreement.

Data obtained from disdrometer can be used to show that the droplet radius follows a modified Gamma distribution. The modified Gamma distribution can be expressed as follows:

$$n(r) = Lr^{\left(\frac{1}{b}-3\right)}e^{-r/ab}, \qquad (1)$$

$$r > 0, \quad a > 0, \quad and \quad 0 < b < 1/2$$

where *r* is the radius of a water droplet, assuming that the water droplets have a spherical shape; *a* and *b* are the parameters of the probability distribution function, and *L* is a scaling constant that is necessary for a probability distribution function. That is, in order to be a probability density function the following integral must be satisfied: $\int_0^\infty n(r)dr = 1$, and so after solving the previous integral it can be shown that $L = \frac{(ab)^{(2-1/b)}}{\Gamma\left(\frac{1-2b}{b}\right)}$, where $\Gamma(m)$ is the Gamma function defined as:

$$\Gamma(m) = \int_0^\infty x^{m-1}\, e^{-x} dx. \qquad (2)$$

The parameter a is called the effective radius and *b* is the effective variance. These parameters have been selected in this way to have a physical interpretation. Thus, to properly interpret the meaning of these parameters, the moment of the k^{th} order of the droplet size distribution will be computed as follows:

$$E(r^k) = \int_0^\infty r^k n(r)dr$$

$$= L(ab)^{\left(k-2+\frac{1}{b}\right)}\Gamma\left(k-2+\frac{1}{b}\right) \qquad (3)$$

Derivation of the formulas is given (Ramirez-Beltran et al., 2009). The expected (average) value of a droplet radius is:

$$E(r) = a(1-2b) \qquad (4)$$

The variance of the water droplet radius, which is the expected deviation of each radius from the typical radius, is:

$$V(r) = a^2b(1-2b) \qquad (5)$$

It should be noted that the effective radius is different from the expected radius and different from the variance of the radius. The effective radius (r_e) is defined as the ratio of the third and second moment of the DSD:

$$r_e = \frac{E(r^3)}{E(r^2)} = a \qquad (6)$$

It should be noted that the effective radius has a geometrical interpretation: it is approximately equal to the ratio of expected volume of a sphere with radius *r* to the expected area of a circle of radius *r*. This, ratio can be computed as follows:

$$\frac{E(V)}{E(A)} = \frac{E\left(\frac{4}{3}\pi r^3\right)}{E(\pi r^2)} = \frac{4}{3}\frac{E(r^3)}{E(r^2)} = \frac{4}{3} r_e \qquad (7)$$

where $E(V)$ is the expected volume and $E(A)$ is the expected area of water droplets that come from a population with a modified Gamma distribution (eq. 1). The *r* is a random variable associated to the radius of each water droplet. Thus, the effective radius can also be defined as follows:

$$r_e = \frac{3}{4}\frac{E(V)}{E(A)} = \frac{3}{4}\frac{\int_0^\infty \frac{4}{3}\pi r^3 n(r)dr}{\int_0^\infty \pi r^2 n(r)dr} \qquad (8)$$

The effective variance can be defined as the ratio of the expected deviation of the radius from effective radius to the second moment of the DSD, and can be expressed as follows:

$$V_e = \frac{\int_0^\infty (r-a)^2 r^2 n(r)dr}{a^2 \int_0^\infty r^2 n(r)dr} = b \qquad (9)$$

It should be mentioned that the extra term r^2 in the numerator and a^2 in the denominator of equation (9) are required to make the V_e dimensionless and a relative measurement of the droplet size variability.

With the purpose of illustration that the droplet radius follows the modified Gamma distribution a 5 minutes data were arbitrarily selected and the corresponding histogram and modified Gamma distribution are shown in Figure 7.

4. Effect of drop size distribution on reflectivity

The studied area is shown in Figure 8, which exhibits the location of the rain gauge, the disdrometer, and the closet 16 radar pixels. Radar provides reflectivity in polar coordinates which were translated into a Cartesian coordinates as shown in Figure 8. Each pixel covers and area of 1km^2.

The NEXRAD level II were used to extract reflectivity values during the same time of the rainfall events recorded by the disdrometer. A computer program was written to compare reflectivity data from the NEXRAD and from disdrometer.

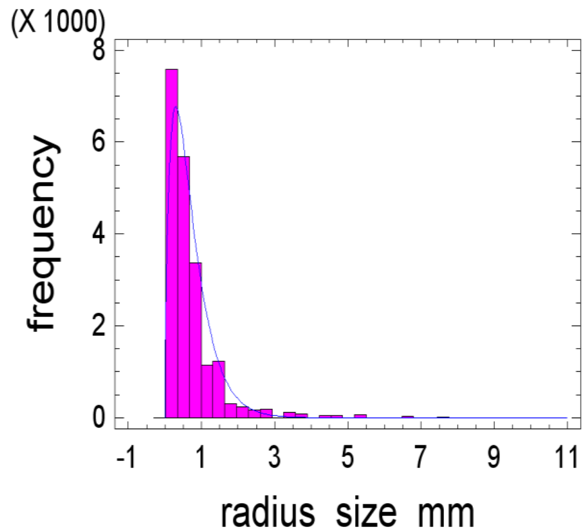

Fig 7. *The modified Gamma distribution. The estimates of the distribution are*: $a = 1.51mm$, $b = 0.27$, $E(r) = 0.70mm$, and the $V(r) = 0.28$.

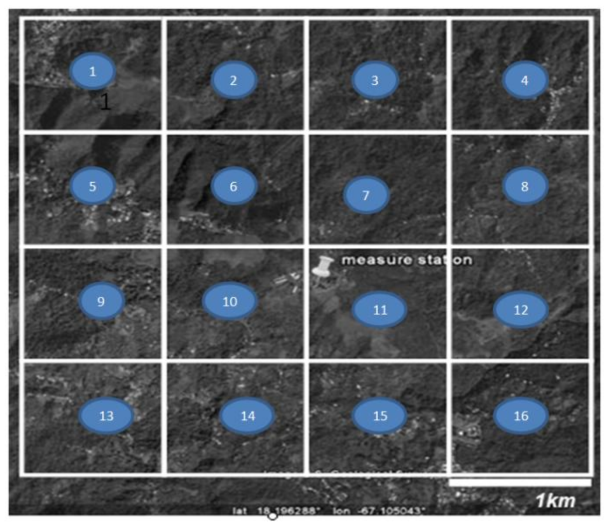

Fig 8 *The closest 16 NEXRAD pixels to the disdrometer. The clip shows the location of disdrometer and rain gauge.*

The data were organized in three classes depending of the average of the droplet radius. The first class includes radius with average less than 0.4mm, the second class when the radius is equal and larger than 0.4 and less than 0.6mm, and the third class corresponds to radius equal or larger than 0.6mm. The classifications of the droplets radius are given in Table 1. Reflectivity values smaller than 10 decibels were eliminated since the rainfall associate is very small and it may correspond to noise information. Reflectivity values larger than 50 decibels are also considered as instrument errors.

The surface reflectivity values measured by the disdrometre were compared with volumetric reflectivity values measured by NEXRAD. Preliminary results show that the deviation of radar reflectivity form disdrometer reflectivity increases as the average of the droplet size is larger, and results are given in Table 1.

Table 1. Average deviation between disdrometer and radar reflectivities

radius	Class	Average Error
$r < 0.4mm$	1	4.37dBz
$0.4 \leq r < 0.6mm$	2	25.35dBz
$r \geq 0.6mm$	3	30.81dBz

Figures 9-11 show the reflectivity measured by disdrometer and radar, for the small, medium and large droplet radius for the rainfall events that occurred on July 2009 in Puerto Rico. In each figure the top panel shows the reflectivity measured by the disdrometer. The central panel shows the average of reflectivity measured by the 16 radar pixels of the radar and the bottom panel presents the absolute value of the deviation between the disdrometer and radar reflectivity.

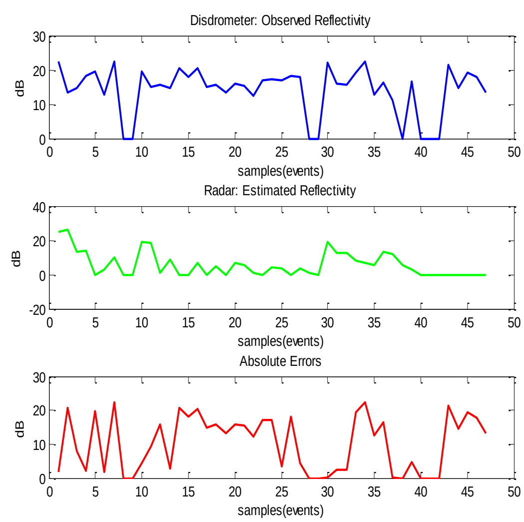

Fig 9. *Reflectivity measured by disdrometer and radar for small droplets.*

5. Future plans and consequences

4.1 Future plans

These preliminary results are based on a small sample size. Thus, an extended work is required to confirm or to modify the preliminary conclusions. Preliminary result show that deviation between the observed reflectivity values at the surface are different from the observed volumetric reflectivity values and the apparently deviation is larger for larger droplet radius. These preliminary results will be verified with another disdrometer that will be installed in the same place, and also the sample size will be increased to derive robust conclusions.

Reflectivity recorded by the NEXRAD may be affected by the elevation of the radar. Earth curvature cause may also cause incorrect estimation of the rain rate. Thus, future work will be dedicated to derive a bias correction factor to improve the radar ran rate estimates.

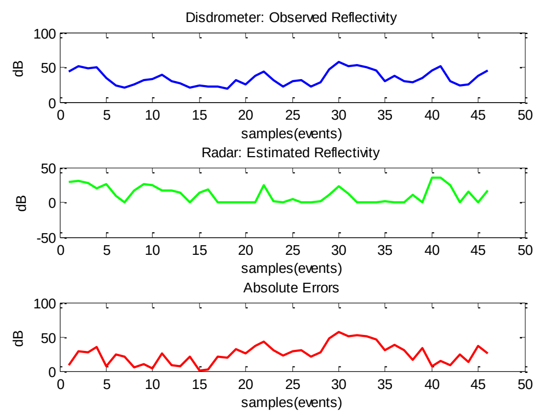

Fig 10. *Reflectivity measured by disdrometer and radar for medium droplets.*

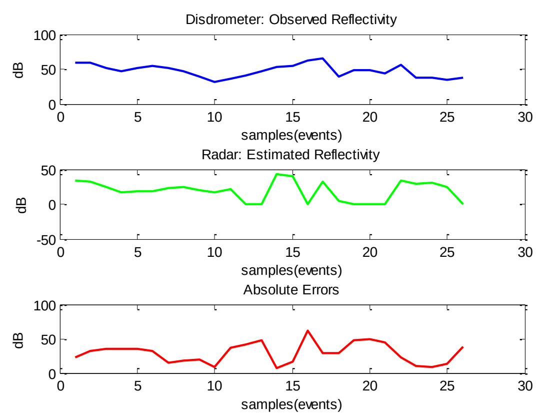

Fig 11. *Reflectivity measured by disdrometer and radar for large droplets.*

Acknowledgements.

This research has been supported by the NSF-ERC-CASA with a grant Number 0313747, NOAA-NWS grant number NA06NWS468001, and also by the University of Puerto Rico at Mayagüez. The authors appreciate and recognize the funding support from these institutions.

References

Arduini, R.F., P. Minnis, W.L. Smith Jr., J.K. Ayers, M.M. Khaiyer, and P. Heck, 2005. Sensitivity of Satellite-Retrieved Cloud Properties to the Effective Variance of Cloud Droplet Size Distribution. *Fifteen ARM Team Meeting Proceedings*, Daytona Beach, FL. 1-13.

Clack, W.L, K.S. Gage, C.R. Williams, P Johnston, and D. Carter. Moveable UHF/S-Band Profiler/Disdrometer Systems as a Calibration Standard in Rainy Places. Tenth International Workshop on Technical and Scientific Aspects of MTS Radar-MTS10. Universidad de Piura, Northern Peru, 13-20 May 2003.

Hansen, J.E., 1971. Multiple scattering of polarized light in planetary atmospheres, Part II. Sunlight reflected by terrestrial water clouds. *J. Atmospheric Sciences*. **28**, 1400-1426.

Nakajima, T., and M.D. King, 1990. Determination of the Optical Thickness and Effective Particles Radius of Clouds from Reflected Solar Radiation Measurements. Part I: Theory. *J. Atmospheric Sciences*, **47**, 15, 1878-1893.

Ramírez-Beltran, N.D, Kuligowski, R.J., Cardona-Soto, M, Cruz-Pol, S. (2009). Warm Rainy Clouds and Droplet Size Distribution. *WSEAS Transaction on Systems*. Vol. 8, Issue 1, pp 75-85.

Yang, P., K.N. Liou, K. Wyser, and Mitchell, 2000. Parameterization of the scattering and absorption properties of individual ice crystals. *J. Geophys., Res*. 105, 4699-4718